Tellus (1981), *33*, 428–437

Characteristic anomaly patterns of summer sea-level pressure for the Northern Hemisphere

By T. J. BLASING, *Environmental Sciences Division, Oak Ridge National Laboratory, Oak Ridge, TN 37830, U.S.A.*

(Manuscript received June 30; in final form December 30, 1980)

ABSTRACT

Characteristic type patterns of Northern Hemisphere sea-level pressure anomaly for summer (July–August) were identified by analyzing the pressure departure maps for the 77 summers from 1900 through 1976, using a pattern recognition algorithm based on the use of the correlation coefficient to measure similarity between map patterns. The procedure allows assessment of statistical significance of the anomaly for each data point on each type pattern. Six types were identified, and the first four of these contained over 93% of those anomalies which were significant at the 99% confidence level. Significant anomalies occurred least frequently in middle latitudes, rather than at low latitudes where the standard deviations of the actual departure values are smallest.

The two most prominent type patterns have approximately the same configuration, but with opposite anomaly signs. Observed pressure anomaly patterns resembling the first type tended to occur during the period of relatively high mean annual Northern Hemisphere surface temperature, from about 1925 to 1955. Anomaly patterns resembling the second type occurred mainly before 1920, when the mean annual Northern Hemisphere temperature was lower than it has been since. The third and fourth type patterns suggest modes of covariance between the "monsoon" circulation in southeast Asia and its less dramatic counterpart in the southwestern United States.

1. Introduction

One way to study climatic change over a large region is to identify characteristic spatial patterns of climatic anomaly and then to represent the degree of similarity between a characteristic pattern and each of the actual patterns in a temporal sequence. Pattern recognition methods can be used to objectively identify general patterns that appear often, such as above-normal winter temperatures in the western United States together with below-normal temperatures in the East. The basis for the map-pattern correlation method used in this study was first described by Lund (1963) who applied it to classify a large number of daily weather maps into a small number of "weather types". Blasing (1975a) modified the method for climatic studies and compared it to principal component eigenvector analysis, which produces orthogonal characteristic anomaly patterns, thereby reducing variance in a statistically efficient fashion. However, by being statistically efficient, the procedure grouped two distinct climatic anomaly types into one eigenvector, rather than distinguishing between the types. This result of Blasing (1975a) is also discussed by Blasing and Lofgren (1980), who used the map-pattern correlation method in their description of characteristic climatic anomaly patterns over the North Pacific sector and western North America during the 20th century. The specific pattern-recognition algorithm used in this study was described in more detail, and used to analyze winter patterns of Northern Hemisphere sea-level pressure anomaly by Blasing (1979).

The purposes of this paper are to briefly describe the pattern recognition method used, to describe its application to the analysis of sea-level pressure anomaly patterns over the Northern Hemisphere for 20th-century summers, and to discuss some implications of the results for future climatic

0040-2826/81/040428-10$02.50/0

studies. One such implication is that identifiable, hemispheric-scale, patterns of atmospheric circulation anomaly correspond to variations of Northern Hemisphere temperature apparent in the data of Brinkmann (1976). Relationships between Northern Hemisphere temperature and regional climatic anomalies were suggested by Namias (1980) and Blasing and Lofgren (1980). Investigation of such relationships is relevant to current concerns about global-scale temperature changes that may result from human activity, such as a CO_2-induced warming of the troposphere (Manabe and Wetherald, 1980).

The type of work reported here falls under the analysis phase in the more general context of the scientific method. Specific causal mechanisms are not investigated. The goal of this type of work is perhaps best expressed by Kutzbach (1970) as follows. "It is mainly useful in helping to isolate both spatial regions and times of particular interest that may then be studied by more suitable techniques."

2. Data and region of analysis

The data set used here was derived from the monthly mean values of sea-level pressure at selected grid intersections for the Northern Hemisphere, available from the National Center for Atmospheric Research. The 180 grid intersections included in this analysis are distributed as follows. At latitudes 20°, 30°, 40°, and 50° N, grid points are spaced at intervals of 10° longitude beginning with the Greenwich Meridian, but at latitudes 60° and 70° N, the longitude interval changes to 20° to compensate for the crowding of data points due to the convergence of meridians. These are the same 180 data points used by Kutzbach (1970) in his study of Northern Hemisphere pressure patterns. This analysis covers only latitudes 20° to 70° N, because data for large regions outside of that latitude range are not available. Occasional missing data at grid points included in the analysis were estimated by linear interpolation of values at surrounding grid points.

Problems with this Northern Hemisphere pressure data set have been discussed by Williams and van Loon (1976). Abrupt shifts in the level of the pressure values at some grid points, usually occurring at 1940, have been noted by those authors and also by Madden (1976). There is also a problem in parts of the Arctic, where early observations are scarce and estimated values of pressure may have been too high. Results of this study, and others based on the same data set, should be interpreted with these problems in mind.

The 77 summer pressure patterns analyzed include those from 1900 through 1976. July and August pressure values were averaged for each summer at each grid point to obtain the series of summer mean maps. The selection of July and August as the summer months, rather than the more conventional period which also includes June, was based on previous work by Bryson and Lahey (1958) and more recent work by Blasing (1975b).

The mean pressure map for any one summer will closely resemble that for other summers, but anomaly maps clearly show how one summer differs from another. Therefore, the long-term (1900–1976) mean summer pressure at each grid point was subtracted from the corresponding actual value, for each summer, to produce the 77 pressure anomaly maps which were then analyzed as discussed below.

3. The map pattern correlation technique

The method outlined in the following paragraphs is based on the use of the correlation coefficient between two map patterns as a measure of their similarity. Similar map patterns can be grouped into a single type, and several types can be found in one data set. The number of types will depend on the level of generality desired in the types, as prescribed by the investigator. This level of generality, g, is simply the number of map patterns that will be averaged to obtain a type pattern. For example, if n is the total number of maps to be analyzed, then the ultimate level of generality is $g = n$. In that case, all maps are averaged to produce only one type, which is the average map. (For a set of anomaly maps, the average is a map of zeroes.) Alternatively, the ultimate level of specificity is $g = 1$, and each map pattern is its own type. The goal of this analysis is to identify types of map patterns that lie somewhere between these two extremes, having more specificity than a mean map but still permitting generalizations about individual case studies or the pressure maps involved. The value of $g = 10$ was found satisfactory for use in a similar analysis of winter pressure maps (Blasing, 1979), and that value is used here also. The computational algorithm is outlined below.

Consider a series of n consecutive maps which show the spatial distribution of some variable, X, based on observations at m locations. The correlation coefficient, r, between the m values for map i and the corresponding m values for map j is

$$r_{i,j} = \sum_{k=1}^{m} (x_{i,k} - \bar{x}_i)(x_{j,k} - \bar{x}_j)$$

$$\times / [\sum_{k=1}^{m} (x_{i,k} - \bar{x}_i)^2 \sum_{k=1}^{m} (x_{j,k} - \bar{x}_j)^2]^{1/2} \quad (1)$$

where $x_{i,k}$ and $x_{j,k}$ are observations at the m corresponding points on maps i and j, and $\bar{x}_i$ and $\bar{x}_j$ are the averages of the m values on map i or map j, respectively. The correlations between each map pattern and every other map pattern are arranged as the elements of the n by n matrix, R, in which the correlation of map pattern j with map pattern i is in column j of row i. Each row of R corresponds to one map pattern such that each element of row i is a correlation coefficient between map pattern i and one of the others (except along the main diagonal where a 1 occurs representing the correlation with itself), and all correlation coefficients involving map pattern i are contained in row i.

Once the correlation matrix, R is determined, the positive values in each row are summed, and the row with the largest sum is identified. The corresponding map pattern and the $g - 1$ others with which it is most highly correlated are averaged to form the first type pattern. All of the $g - 1$ highest correlation coefficients used to identify the corresponding map patterns are printed out for later inspection, and the smallest of these, r_s, is retained for later use. Once the first type pattern is determined, then all map patterns with which it is highly correlated are removed from the data and the process is repeated to find succeeding types. A "high correlation coefficient" is defined for this purpose as any value equal to or above r_s. When r_s is so used, only one number, g, needs to be specified by the investigator, and all other decisions are made within the computational algorithm. The effects of varying g are discussed elsewhere (Blasing, 1979).

4. Results and discussion

Six types of pressure pattern had been identified when the computations were stopped because the number of map patterns that had not been classified into any type (9) was less than g (10). Each pressure anomaly type represents a characteristic mode of departure from the mean pattern of the period analyzed. Contour maps of the mean and standard deviation of summer pressure, over the 77 summers analyzed, are shown in Fig. 1.

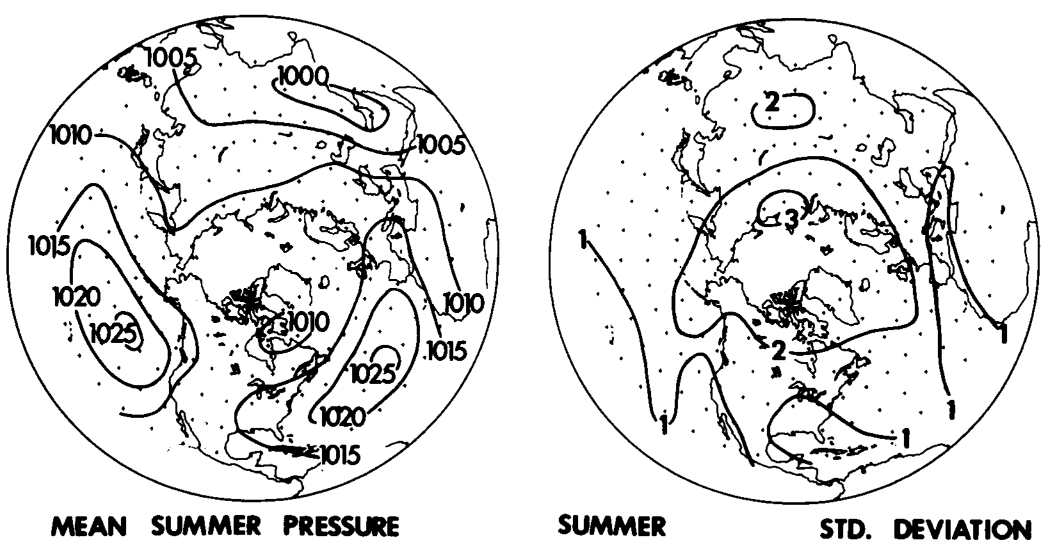

Fig. 1. Mean and year-to-year standard deviation of summer sea-level pressure, for the period 1900–1976, contoured at 1-millibar intervals on a polar, equal-area projection.

Pressure anomalies at each grid point on a type map represent the average of ten departure values, and a two-tailed Student t test was performed at each grid point for each type to determine whether the averaged departure of the 10 values was sufficiently large, relative to their standard deviation, to be significantly different from zero. Of the 1080 values of pressure anomaly contained in the six type patterns (180 locations × 6 maps), more than 10% (109) were statistically significant at the 99% confidence level. This was not considered particularly remarkable because the analysis is descriptive rather than predictive. However, the latitudinal distribution of significant values was somewhat surprising. This distribution is summarized in Table 1, which shows that the number of significant anomalies is greatest in the southern and the extreme northern portions of the study area and lowest in middle latitudes.

Spatially coherent, or organized features of the pressure anomalies might be expected to show up most clearly in middle latitudes, because data from all points in and around any mid-latitude feature are included in the analysis. Large-scale anomaly features at high or low latitudes might be bisected by the boundary of the study area. Such features would not be completely represented in the data and, therefore, would not be expected to show up completely in the analysis. From this consideration alone, it would be easiest to explain a distribution of significant anomalies having a maximum at middle latitudes. However, the actual distribution has a minimum there, so other considerations must apply.

Table 1. *Number of points at each latitude for which an averaged departure in a type pattern was significant at the 99% level, compared to the number of grid points included in the analysis at the corresponding latitude*

A Latitude	B Number of grid points included	C Number of significant values for types 1–6	D Ratio of column C to column B
70° N	18	22	1.22
60° N	18	8	0.44
50° N	36	8	0.22
40° N	36	19	0.53
30° N	36	21	0.58
20° N	36	31	0.86
	$\Sigma = 180$	$\Sigma = 109$	

The large number of significant anomalies at high latitudes could be partially due to systematic errors in the interpolation of some of the Arctic data in the early portion of the record. However, it is seen in Fig. 1 that the summer-to-summer variance of pressure increases roughly as does the latitude, even in regions of relatively good-quality pressure data. Significant pressure anomalies for a given type are most likely to show up where the variance for the entire 77-year period is large compared to the variance for only those summers of the type.

The tendency for significant anomalies at low latitudes was particularly surprising because the summer pressure values have little variance compared to those at higher latitudes (Fig. 1). The statistical significance of the pressure anomalies at low latitudes cannot easily be attributed to systematic data (interpolation) errors, because such errors would be most likely to show up in mid-ocean areas. However, the distribution of statistically significant anomalies at low latitudes showed no such preference. Many of these anomalies occurred in or near populated continental areas, where land-based temperature and precipitation records are likely to be available for further climatic analysis.

Fig. 2 shows the number of points (out of 180) in each type pattern for which the averaged departure was significant, at both the 95 and 99% levels. The number of grid points with significant anomalies is relatively constant for each of the first four types, but drops off noticeably for types 5 and 6. Therefore, in this discussion the emphasis will be on the first four types.

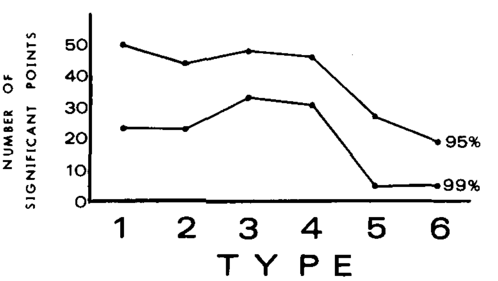

Fig. 2. The number of points at which the pressure anomaly is significantly different from zero, at both the 95 and 99% confidence levels, on each of the six type patterns.

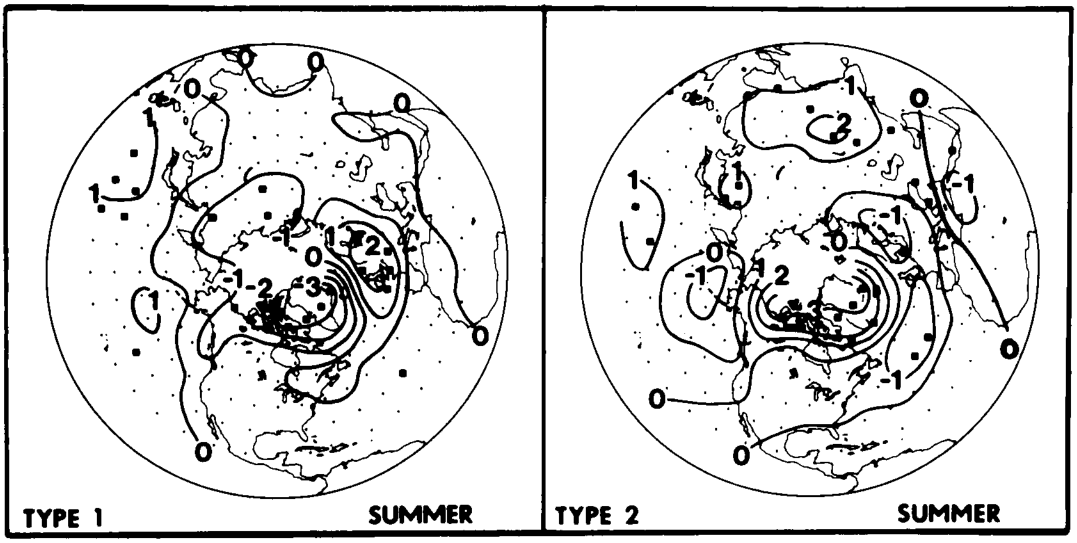

Fig. 3. Summer pressure anomaly types 1 and 2 for the Northern Hemisphere (polar, equal-area projection). Contours are at 1-millibar intervals. Black squares indicate points at which the anomaly is significantly different from zero at the 99% confidence level.

Maps of the first two pressure anomaly types are shown in Fig. 3. Black squares indicate points at which the pressure anomaly differs significantly from zero, at the 99% confidence level. With the exception of the region of positive pressure anomalies over central Asia in type 2, the first two type patterns are quite similar in configuration, although the anomalies differ in sign from one type to the other. In each of these types, a large region over northwestern Asia has anomalies of the same sign as those over Greenland, while the opposite sign characterizes a region centered near Oslo, Norway and another region centered near, or just south of, the Alaska Peninsula.

Occurrences of observed patterns resembling each of these type patterns are indicated in Fig. 4, which shows the correlation coefficient between the observed anomaly pattern for each summer and the type pattern indicated. A high positive correlation indicates the type was well represented in that summer's pressure anomaly pattern, while a negative correlation implies opposite features, perhaps characteristic of a different type pattern, were present. Type 1, for example, was well correlated with observed patterns during the period of relatively high Northern Hemisphere annual temperature, from roughly the mid-1920s to the mid-1950s. Type 2 was conspicuous by its absence then, but appeared more prominently during the period of relatively low Northern Hemisphere temperature prior to about 1920. Five-year averages of the correlation coefficients representing type 1 in Fig. 4 were computed for

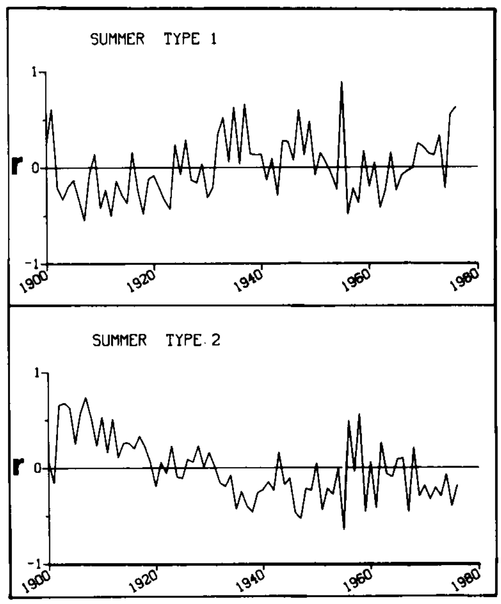

Fig. 4. Correlation coefficient between the type pattern indicated and the observed pressure anomaly pattern for each summer from 1900 through 1976.

comparison with the five-year averages of Northern Hemisphere Temperature (NHT) taken from Brinkmann (1976). The correlation coefficient between the two series of five-year averages is +0.69. The corresponding correlation for type 2 with NHT is −0.84. Two characteristics of spurious correlations (limited number of observations and high serial correlation within each series) are present here. However, these correlations are still quite high, and the spatial configuration of the type patterns involved seems reasonable.

Higher NHTs are characterized by pressure anomaly patterns indicative of expansion of the stationary subtropical high pressure systems, with a northward displacement of the traveling low-pressure systems (type 1). Low NHTs are characterized by opposite features, plus some apparent weakening of the "monsoon low" indicated by positive pressure anomalies over south-central Asia (type 2). Anomalies in the region of the "monsoon low", as occur in type 2 and type 4, may reflect inconsistencies in data reporting as discussed by Williams and van Loon (1976), and should be interpreted cautiously until checked for consistency with temperature and precipitation anomalies in the same region.

Kutzbach (1970) used principal component eigenvector analysis to investigate anomaly patterns of January and July pressure for the Northern Hemisphere. He noted intervals of change in the early to mid-1920s and the early to mid-1950s. Certain circulation patterns were seen to have been relatively prominent over periods of a decade or longer, though with considerable year-to-year variation superimposed. Kutzbach suggested that "slowly changing energy sources or sinks" might be responsible for the tendency of some circulation features to persist or recur frequently "for intervals on the order of a decade or longer", while the shorter-term variations in the pressure anomaly pattern "may reflect variability confined primarily to the atmosphere, or associations with anomalous energy sources and sinks that have little year-to-year persistence".

The same intervals of change in the character of Northern Hemisphere pressure anomaly patterns were noted by Blasing and Lofgren (1980) in their analysis of spring, summer, autumn, and winter climatic anomaly patterns for the North Pacific sector and western North America. The possible relationship of climatic anomalies in that region to the NHTs presented by Brinkmann (1976) was also discussed by Blasing and Lofgren (1980). Namias (1980) used upper air data to investigate relationships between Northern Hemisphere atmospheric circulation patterns and NHT during the period 1951–78.

Intuitively, the general circulation of the atmosphere would be expected to respond to changes in its energy balance, as reflected in NHT trends. The circulation changes would, in turn, affect temperature and precipitation patterns in individual regions. The relationships involved would be expected to evolve in a complex way, over more than one year, because a number of complex feedbacks, including oceanic heat storage, are likely to be involved. Therefore, it might be expected that longer-term variations of NHT are related to changes in the frequency of certain types of pressure anomaly pattern over time scales of decades or longer.

For example, Blasing and Lofgren (1980) noted that one summer pressure anomaly type for the North Pacific sector and western North America, featuring an expanded/intensified Pacific subtropical high, was most prominent over the period of about 30 years when NHTs were the highest in the period of instrumental record. The associated anomalous northerly wind in the Pacific Northwest led to below-normal temperatures in that region, even though most of the United States was warmer than normal when that particular pressure anomaly type was prominent.

The pressure anomaly patterns of types 1 and 2 closely resemble the winter pressure patterns corresponding, respectively, to the GB and GA categorizations of van Loon and Rogers (1978) which, in turn, resemble types 1 and 2, respectively, of winter pressure anomaly presented by Blasing (1979). There is also an obvious similarity between Kutzbach's (1970) first eigenvector pattern of January pressure anomaly and his second eigenvector pattern of July pressure anomaly (with sign reversed). Both of these eigenvector patterns are similar to the pressure anomaly types discussed above. These patterns, similar in configuration but having anomalies of opposite sign, are prominent modes of both summer and winter pressure anomaly for the Northern Hemisphere.

Unfortunately, for long-range prediction, temporal associations between occurrences of similar summer and winter pressure anomaly patterns are not obvious. A particular type of winter does not tend to be selectively followed by a particular type of summer, and particular types of summer do not appear to be followed by any preferred winter patterns. Even on time scales of several years, there is no direct relationship between summer and winter pressure anomalies, but there may be a tendency for an inverse relationship. For example, the data of van Loon and Rogers (1978) indicate that the period 1925–1955, when type 1 summers were most prominent, included only three of the 14 (20th century) cases of GB winter (for which the pressure anomaly pattern is similar to type 1 summer). Also, the period 1900–1920, when type 2 summers were most prominent, included none of the GA winters (for which the pressure anomaly pattern is similar to type 2 summer). In summary, for a period of consistent NHT anomaly the corresponding pressure anomaly features may vary from season to season, and those of winter may even tend to be opposite to those of summer.

This could mean that the recorded NHT variations do not correspond to specific pressure anomaly patterns as clearly as they appeared to from the summer study alone. Alternatively, the reversed land-ocean temperature gradient in winter and the increased south-north temperature gradient, especially prominent over continents, may lead to differences in the way the winter pressure anomaly responds to changes in NHT. The winter circulation may be slower in responding to increased NHT, because that is when lagged effects due to increased vertical mixing of the oceanic surface layer appear to be most prominent (Namias and Born, 1974). More synoptic-climatological studies of the historical record of climate, and the general-circulation-model simulations of climate, are necessary to adequately describe the effects of global-scale temperature changes on the general circulation of the atmosphere.

Types 3 and 4 (Fig. 5) have many significant anomalies at low latitudes, where the summer-to-summer variance of pressure is low (Fig. 1). Both types have a large region of significant pressure anomalies centered roughly over Florida, and a smaller cluster of significant anomalies in the general region of southeastern Asia. For both types, anomalies over the southwestern United States are of the same sign as those over India. Both of these regions are characterized by so-called "summer monsoon" precipitation. The largest pressure anomalies in type 4 are over Siberia. However, some caution should be used in interpreting these particular anomalies, because they may indicate systematic data errors in that sparsely populated area, where interpolation is often necessary to obtain numerical values.

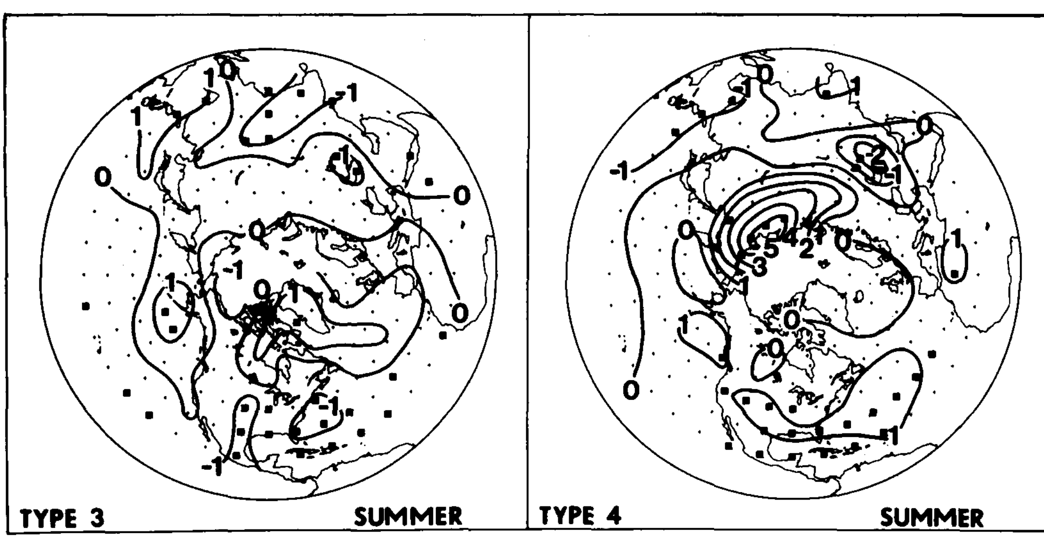

Fig. 5. Summer pressure anomaly types 3 and 4 for the Northern Hemisphere (polar, equal-area projection). Contours are at 1-millibar intervals. Black squares indicate points at which the anomaly is significantly different from zero at the 99% confidence level.

Occurrences of observed patterns resembling types 3 and 4 are indicated in Fig. 6, which shows the correlation coefficient between each observed summer pressure anomaly pattern and the type pattern indicated. Type 3 occurrences were mainly in the last half of the data period. Summers resembling type 4 occurred mainly around 1920, when data errors in Siberia are especially likely to have been a contributing factor.

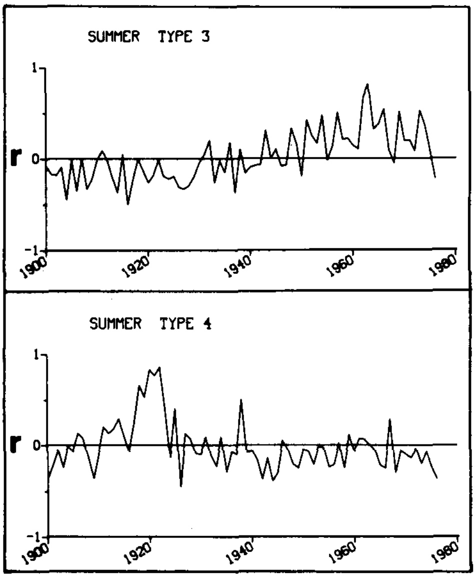

Fig. 6. Correlation coefficient between the type pattern indicated and the observed pressure anomaly pattern for each summer from 1900 through 1976.

Types 5 and 6 (Fig. 7) have anomalies of opposite sign in the 70° latitude region. The three statistically significant anomalies in type 5 are clustered in Siberia. The four statistically significant anomalies in type 6 are scattered. The correlation coefficients between observed pressure anomaly patterns and each of these type patterns are shown in Fig. 8. Type 5 was most prominent in the 1940s and early 1950s; type 6 was most prominent before about 1940. Type 6 should be interpreted with particular caution because 1940 is the first year after a change in the data souree (Williams and van Loon, 1976).

The temporal variation of type 5 (Fig. 8) shows trends which are similar to those of type 1 (Fig. 4). Both types tend to occur during periods of high NHT. Type 5 occurred primarily during the four summers from 1939 to 1942, suggesting the possibility of a temporary problem with data reporting in some regions. Type 1 was conspicuous by its absence then (Fig. 4), which may, in part, be due to the same data problem, if indeed there was a sufficiently critical data problem. Types 1 and 5 both have negative pressure anomalies at high latitudes and positive anomalies centered over

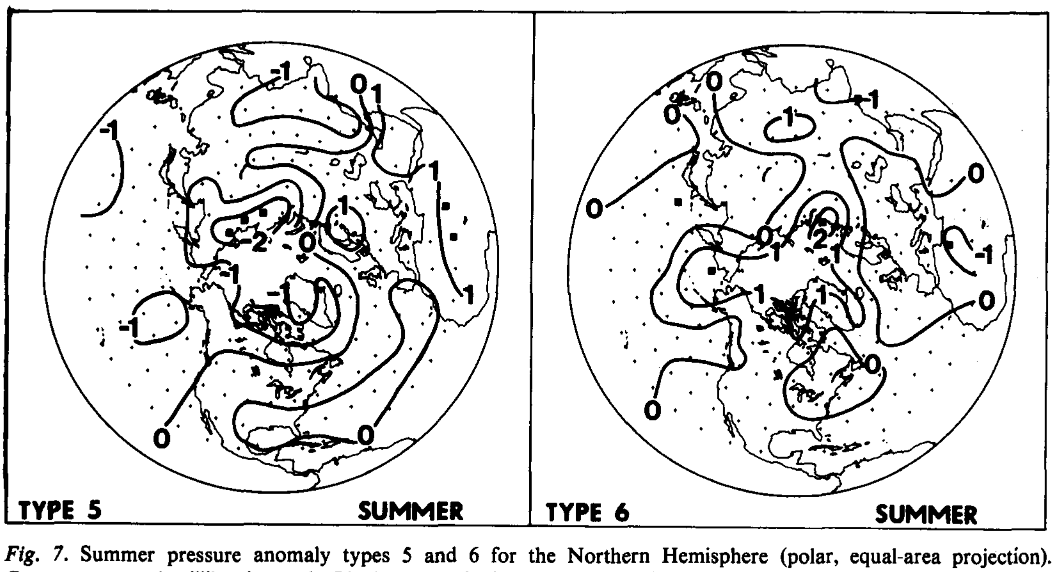

Fig. 7. Summer pressure anomaly types 5 and 6 for the Northern Hemisphere (polar, equal-area projection). Contours are at 1-millibar intervals. Black squares indicate points at which the anomaly is significantly different from zero at the 99% confidence level.

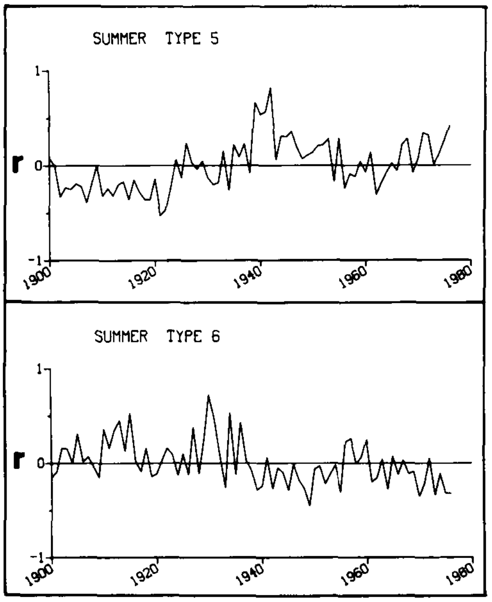

Fig. 8. Correlation coefficient between the type pattern indicated and the observed pressure anomaly pattern for each summer from 1900 through 1976.

northern Europe. They differ in the Pacific where type 5 has negative anomalies and type 1 has positive anomalies, and in the Atlantic where type 5 has positive anomalies located mostly at 30° N and type 1 has positive anomalies located mostly at 50° N.

5. Summary and conclusions

Characteristic type patterns of Northern Hemisphere sea-level pressure anomaly, for the summers from 1900 through 1976, were derived using a map-to-map correlation method as a pattern recognition device. Each type pattern was obtained by averaging values of ten similar anomaly maps at each of 180 grid points. Statistical significance of the averaged departures at each grid point for each type pattern was evaluated with the Student t test. Over 10% of the anomalies were significant at the 99% confidence level. Analysis of the spatial distribution of significant anomaly values provided information which could not have been obtained from analysis of only the magnitudes of the anomalies. In particular, a surprisingly large number of significant anomalies showed up at low latitudes, and relatively few significant anomalies showed up in middle latitudes. Regions frequented by significant anomalies include the southeastern United States and adjacent oceanic areas, Greenland and the Canadian archipelago, Siberia, and southern Asia.

In view of the idiosyncracies in the data set, as noted by Williams and van Loon (1976), and others, it should be kept in mind that some of the pressure anomalies may represent peculiarities of the data reporting systems. When the pressure data accurately reflect a real feature, rather than systematic data errors, then the pressure anomaly feature should be synoptically consistent with anomaly patterns of temperature and precipitation in the same region. This sort of checking is encouraged, wherever possible, before firm conclusions are drawn regarding the nature of some of the pressure anomaly features identified in this initial study. This paper is intended mainly to indicate where to look and what to look for in terms of summer features of atmospheric circulation associated with global-scale climatic variations.

The first two pressure anomaly type patterns are characterized by pressure anomalies of one sign over Greenland and much of northern Canada, and anomalies of the opposite sign south of Alaska and also over a region covering most of Europe and extending across the Atlantic to Newfoundland. These summer patterns were noted to be remarkably similar to winter patterns of pressure anomaly previously presented by others (e.g., van Loon and Rogers, 1978).

The temporal distribution of occurrences of the first two types shows an intriguing correspondence to the Northern Hemisphere surface temperature trend for the 20th century. Pattern recognition techniques may be useful in identifying anomaly features of the atmospheric circulation associated with changes in the magnitude and distribution of energy sources or sinks such as those which may be related to hemispheric-scale warming or cooling. In view of the concern over possible effects of technological activity on climate (e.g., increases in atmospheric carbon dioxide), this topic merits further attention.

6. Acknowledgments

I wish to thank R. G. Barry, J. R. Carter, and J. S. Olson, who read early drafts of this paper and provided many helpful comments. I also thank Julie

Watts for her assistance with the computational and data management aspects of this work. This research was sponsored by the Division of Environmental Research, CO_2 Effects Research Program, U.S. Department of Energy, under contract W-7405-eng-26 with Union Carbide Corporation. Publication No. 1663, Environmental Sciences Division, ORNL.

REFERENCES

Blasing, T. J. 1975a. A comparison of map pattern correlation and principal component eigenvector methods for analyzing climatic anomaly patterns. In *Preprint Volume, Fourth Conference on Probability and Statistics in Atmospheric Sciences*. Boston/U.S.A.: American Meteorological Society, 96–101.

Blasing, T. J. 1975b. Methods for analyzing climatic variations in the North Pacific sector and western North America for the last few centuries. Ph.D dissertation, Department of Meteorology, University of Wisconsin, Madison, Wisconsin, U.S.A., 177 pp.

Blasing, T. J. 1979. Map pattern classification at a prescribed level of generality. In *Preprint Volume, Sixth Conference on Probability and Statistics in Atmospheric Sciences*. Boston/U.S.A.: American Meteorological Society, 118–125.

Blasing, T. J. and Lofgren, G. R. 1980. Seasonal climatic anomaly types for the North Pacific sector and western North America. *Mon. Wea. Rev. 108*, 700–719.

Brinkmann, W. A. R. 1976. Surface temperature trend for the Northern Hemisphere—updated. *Quat. Res. 6*, 355–358.

Bryson, R. A. and Lahey, J. F. 1958. The march of the seasons. Final Report AF 19(604)992, Department of Meteorology, University of Wisconsin, Madison, Wisconsin/U.S.A., 41 pp.

Kutzbach, J. E. 1970. Large-scale features of monthly mean Northern Hemisphere anomaly maps of sea-level pressure. *Mon. Wea. Rev. 98*, 700–716.

Lund, I. A. 1963. Map pattern classification by statistical methods. *J. Appl. Meteor. 2*, 56–65.

Madden, R. A. 1976. Estimates of the natural variability of time-averaged sea-level pressure. *Mon. Wea. Rev. 104*, 942–952.

Manabe, S. and Wetherald, R. T. 1980. On the distribution of climate change resulting from an increase in CO_2 content of the atmosphere. *J. Atmos. Sci. 37*, 99–118.

Namias, J. 1980. Some concomitant regional anomalies associated with hemispherically averaged temperature variations. *J. Geophys. Res. 85*, 1585–1590.

Namias, J. and Born, R. M. 1974. Further studies of temporal coherence in North Pacific sea surface temperatures. *J. Geophys. Res. 79*, 797–798.

van Loon, H. and Rogers, J. C. 1978. The seesaw in winter temperatures between Greenland and northern Europe. Part I: general description. *Mon. Wea. Rev. 106*, 296–310.

Williams, J. and van Loon, H. 1976. An examination of the Northern Hemisphere sea-level pressure data set. *Mon. Wea. Rev. 104*, 1354–1361.

ТИПОВЫЕ ШАБЛОНЫ ПОЛЯ АНОМАЛИЙ ДАВЛЕНИЯ НА УРОВНЕ МОРЯ В СЕВЕРНОМ ПОЛУШАРИИ ДЛЯ ЛЕТНЕГО СЕЗОНА

Получены характерные шаблоны поля аномалий давления на уровне моря для летнего сезона/июль-август/путем анализа карт аномалий давления для 77 летних сезонов с 1900 по 1976 г. с помощью алгоритма распознавания изображений, основанного на использовании коэффициента корреляции, как меры подобия между шаблонами. Эта процедура позволяет оценивать статистическую значимость аномалии для любого пункта и каждого шаблона. Установлено, что имеется 6 типов шаблонов, причем первые 4 из них содержат свыше 93% тех аномалий, которые значимы на 99—процентном уровне значимости. Значимые аномалии наименее часто повторяются в средних широтах, а не в низких широтах, где стандартные отклонения фактических аномалий наименьшие. Два наиболее важных шаблона имеют сходную конфигурацию, но знаки аномалий у них противоположны. Наблюдаемые поля аномалий давления, принадлежащие первому типу, преимущественно относятся к периоду относительно высокой среднегодовой наземной температуры северного полушария—приблизительно с 1925 по 1955 г. Поля аномалий второго типа встречаются в основном до 1920 г., когда среднегодовая температура северного полушария была ниже, чем она стала впоследствии. Третий и четвертый типовые шаблоны указывают на существование корреляции между "муссонной" циркуляцией в юго-восточной Азии и менее ярко выраженной сходной циркуляцией на юго-западе США.